Enhanced Photocatalytic Hydrogen Production of Fe₂O₃ Decorated TiO₂ Nanorods: Optimization of Hydrothermal Temperature

Huaiyuan Long[1], Dichen Tan[1], Song Wang[1,], Zuwen Wang[2], Yu Deng[3], Shunyuan Zhang[4]*

[1] School of chemical and environmental engineering, Yangtze university, Jing zhou, Hubei, China.
[2] Chuanqing Drilling Engineering Company Underground Operation Company, Xian, Shanxi, China.
[3] Chuanqing Drilling Engineering Company Drilling Fluids Company, Cheng du. Sichuan, China
[4] China National Petroleum Corporation Engineering Technology Research Institute Co., Ltd, Beijing, China.
[*]E-mail: 1508871707@qq.com and h18872961770@163.com

We developed a nanocomposite of Fe₂O₃ and TiO₂ nanorods (NRs) as a photocatalyst in a photoelectrochemical hydrogen production system through two steps hydrothermal technique. The influence of hydrothermal temperature (100, 120, 150, 180, and 200°C) was investigated on the physicochemical and photoelectrochemical properties and solar hydrogen production of all photocatalysts by various characterization techniques. At low temperatures, nanorods grow irregularly with low concentration due to the insufficient heat however the samples completely peeled off and nanorods were not detected on the glass substrate at temperature 200°C. The photocatalyst with the hydrothermal temperature of 150 °C produced the maximum amount of hydrogen (171.6 mmolcm⁻²) under visible light with external potential of 0.7 V in 1M KOH and 5 vol.% methanol solution. Electron Impedance spectroscopy (EIS) results show that this photocatalyst had a reduction in charge transfer resistance and charge carrier recombination rate due to small inner surface area with low reaction sites. Also, its Mott−Schottky data revealed a more negative flat bad potential of -0.9 V with profound ability of proton (H⁺) reduction to H₂ and a high donor density of 8.45×10^{20} cm⁻³ with a great photocurrent density.

1. INTRODUCTION

The depletion of fossil fuels and climate change are the main reasons for researchers and scientists to focus their attention on clean renewable energy resources. Hydrogen as a great energy carrier with high calorific and without greenhouse gases emission during the combustion process is a

promising alternative for the development of low carbon emission energysource. However, hydrogen production with conventional techniques involves burning of fossil fuels with a large amount of carbon dioxide (CO_2) emission[1]. Combing solar energy with water as clean and abundantly available renewableenergy resources is promising approach to produce hydrogen [2, 3].Scientists across the world obsessed with finding a highly efficient method of generating hydrogen from splitting water in the presence of sunlight through electrolysis process[4]. In 1972, Fujishima and Honda used semiconductor-based photocatalyst in photo-electrochemical cell (PEC), to split the water just like in an electrochemical cell[5]. The general water photosplitting happens by producing photoexcited electron-hole pairs by absorbingsolar energy larger than the bandgap energy, migrating the photoexcited electrons to the surface of photocatalyst and put positive holes behind, and followed by redox reactions to produce hydrogen and oxygen [6-8].To produce hydrogen in a single PEC cell, photocatalyst should have band energy of ~2eV, negative flat band potential and conduction band potential and high stability to chemical and petrochemical corrosion[9-11]. Metal sulphides (CdS) and oxides (TiO_2, ZnO, Fe_2O_3, SiO_2 and WO_3) as n-type semiconductors have been reported as the most efficient photocatalyst materials for photocatalytic solar hydrogen production[12]. TiO_2 with unique characteristics like abundance, high chemical stability, and suitable conduction band has been considered as an attractive photocatalyst for PEC cell. It has been reported that the properties of one-dimensional (1D) TiO_2showed better performance compered to TiO_2 nanoparticles due to direct transport pathways for charge carriers and a great light absorption and scattering[13]. Nonetheless, its photocatalytic is diminished due to its wide band energy, low specific surface area, and presence of single phase of TiO_2[14]. Ferric oxide (Fe_2O_3) with a band gap of 2.2 eVcan absorb wide range of solar spectrum however its low conductivity and high charge carrier recombination rate harm its practical photocatalytic applications. To construct a heterostructure of Fe_2O_3 and $TiO_2$with their suitable valence band and conduction band positions can improve charge carrier separating and transporting and then photocatalytic activity of TiO_2[15]. It is noteworthy to mention that preparation parameters play an important role with agreat influence on the morphologies and the alignment ordering of 1D TiO_2. In this study we applied hydrothermal method to synthesis of Fe_2O_3 and TiO_2 nanocomposite. hydrothermal growth temperatureand reaction time can strongly affect the morphologies of Fe_2O_3 and TiO_2 nanocomposite. However, there is no study on the effect of this parameters on photoelectrochemical and physicochemical properties of the heterojunction Fe_2O_3/TiO_2nanocomposites.

The goal of this research work is to study the effect of varying hydrothermal temperature (100, 120, 150, 180, and 200 °C) on the physicochemical and photoelectrochemical properties and solar hydrogen production of Fe_2O_3/TiO_2 nanorod as photoanode in the PEC cell.

2. EXPERIMENTAL SECTION

2.1. Preparation of Fe_2O_3 doped TiO_2 NRs Thin film

First, the TiO_2 nanorods were prepared by combing deionized (DI) water, concentrated hydrochloric acid (HCl, 37%), and titanium (IV) butoxide (97%) and stirring for 3h at room temperature. A cleaned glass substrate deposited with fluorine-doped tin oxide (FTO) was subsequently dipped in the solution and treated at 100, 120, 150, 180, and 200°C for 12h in a Teflon-lined autoclave. The autoclave was then gradually cooled and followed with rinsing and drying the samples at room temperature. In the second step, TiO_2 NRs was immersed in a mixture of iron (III) chloride (0.03 M) with sodium nitrate (0.2 M) and followed with hydrothermal treatment at 100 °C for 12h, rinsing with DI, and calcination at 500 °C for 2h. These samples were labelled as Fe_2O_3/TiO_2-100, Fe_2O_3/TiO_2-120, Fe_2O_3/TiO_2-150, and Fe_2O_3/TiO_2-180.

2.2. Characterization

X'Pert3 powder and Empyrean, PANalytical was utilized to investigate the crystal structure of prepared photocatalysts at an angle of 2θ from 20 to 80°. Field emission scanning electron microscope (FESEM) (Zeiss Supra 55VP instrument) with a magnification of 10kX was employed for surface morphology study. Diffuse Reflectance- UV-Vis (DR-UV-Vis) was measured using Cary100 spectrophotometer with a wavelength range from 200 to 800 nm[16, 17].
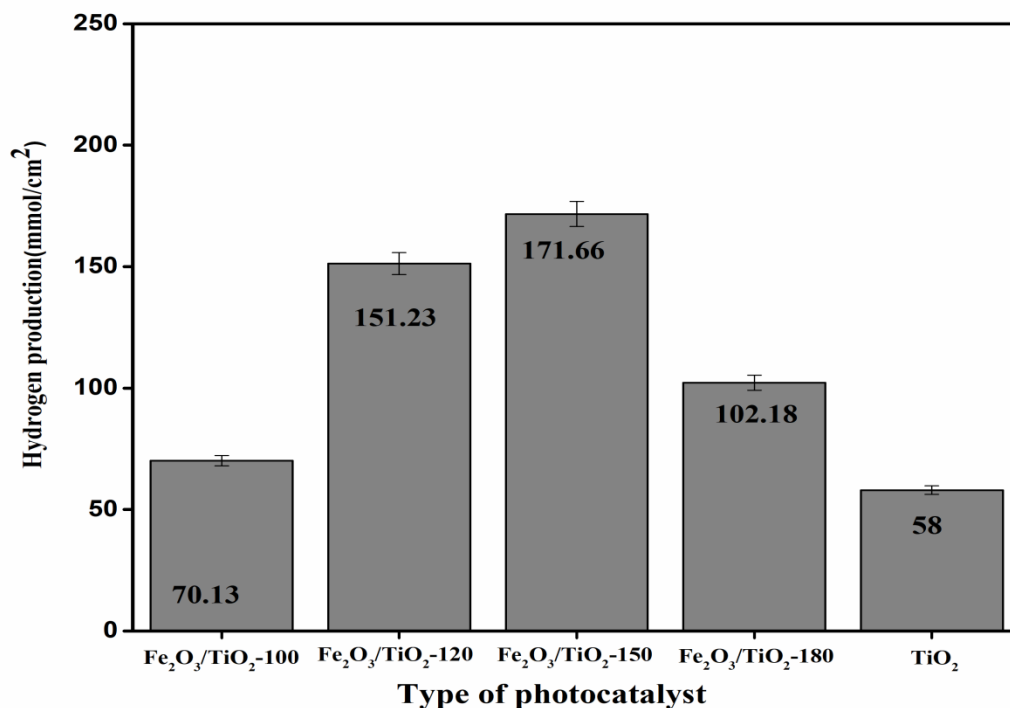
2.3. Photocatalytic study

The photoelectrochemical behaviour and photocatalytic hydrogen production were investigated in 300 mL glass reactor with a mixture of 1M of KOH and methanol solution and Fe_2O_3/TiO_2 nanorods, Pt, and Ag/AgCl in 3M KCl as working, counter, and reference electrodes, respectively undera 500W halogen lamp with an intensity of 100 mW/cm². The three electrode configuration system was applied to study electrochemical impedance spectroscopy (EIS) measurements, Mott−Schottky (M-S), and photocurrent density (jp) via a potentiostate (Autolab PGSTAT302N, Metrohm), thatcame with a frequency response analyzer (FRA) module [18].

3. RESULTS AND DISCUSSION

3.1. Quantification of H_2 evolution

Figure 1 shows that the pure TiO_2 produce 58 mmol/cm² in the photoelectrochemical cell by applying the external bias of 0.7 V. In addition, this results confirm that introducing Fe improved solar hydrogen production. A gradual increase in hydrogen production from 70.13 to 171.66 mmol/cm² was

dpecited byincreasing temperature from 100 to 150 °C. However, a further increase in hydrothermal temperature until 180 °C had a slightly negative effect on the hydrogen production and it had dropped to 151.23 mmol/cm^2. We were not able to detect hydrogen for prepared sample at 200 °C owing to peel off thin film from the substrate. In the following section we do further discussion to explain the influence of hydrothermal temperature on physicochemical properties and photoelectrochemical behaviour properties to control photocatalytic hydrogen production.

Figure 1. Photocatalytic hydrogen production over Fe$_2$O$_3$/TiO$_2$ NR at different hydrothermal temperatures for 2h

Figure 2 shows the XRD patterns of different TiO$_2$ decorated with Fe$_2$O$_3$ at different hydrothermal temperatures. The FTO glass substrate has peak at 26.61, 37.91, and 51.69° of 2θ as identified in Figure 2. The peaks at 2θ values of 36.24°, 61.84.60°, 63.02°, 65.52°, and 70.13° are in good match with the characteristic peaks of (011), (002), (130), (221) and (112) planes of the rutile phase of TiO$_2$ (JCPDS no. 98-020-2241). A peak at 33.22° appeared, by introducing Fe on the surface of TiO$_2$ corresponding to 015 plane of Fe$_2$O$_3$ (JCPDS 98-009-6077) [19, 20]. The intensity of all peaks increased by increasing the hydrothermal temperature from 100 to 150 °C and reached its highest peak when the sample growth temperature is 150 °C. Further increasing the growth temperature resulted in

more nanorods start to grow along (011) direction and the intensities of other TiO_2 rutile and FTO peaks decreases.
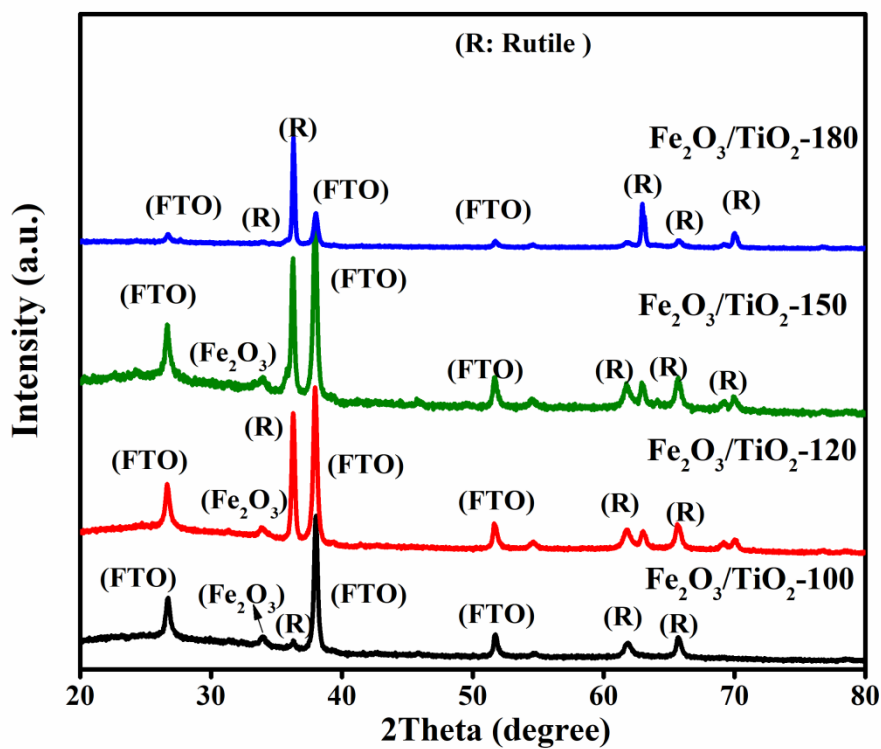
Figure 2. XRD diffraction patterns of Fe_2O_3/TiO_2NRs prepared at different hydrothermal temperatures

The influence of different hydrothermal temperatureson the surface morphology of Fe_2O_3/TiO_2 nanorod photocatalyst are displayed in Figure 3. At low temperature from 100 to 150 °C, the nanorod irregularly grow with low concentration, attributing to low reaction speed and followed by low nucleation and growth rate. Moreover increasing temperatures up to 180 °C resulted in growth of regular nanorod with high concentration. Further increasing temperature up to 200 °C harmed the growth of nanorod and the layer was peeled off from glass surface due to high pressure and rapid hydrolysis process [21].Figure 4 shows that the hydrothermal temperature can strongly effect on the length and diameter of nanorods.Increasing hydrothermal temperature from 100 to 180 °Crapidlyincrease the average length and diameter of TiO_2 nanorods rapidly from 0.409 to 3.47μm and 0.17 to 0.268 μm, respectively. Drawing a comparison, these results show that increasing temperature had causedTiO_2 nanorod to grow towards axial direction rather than radial direction [22, 23].
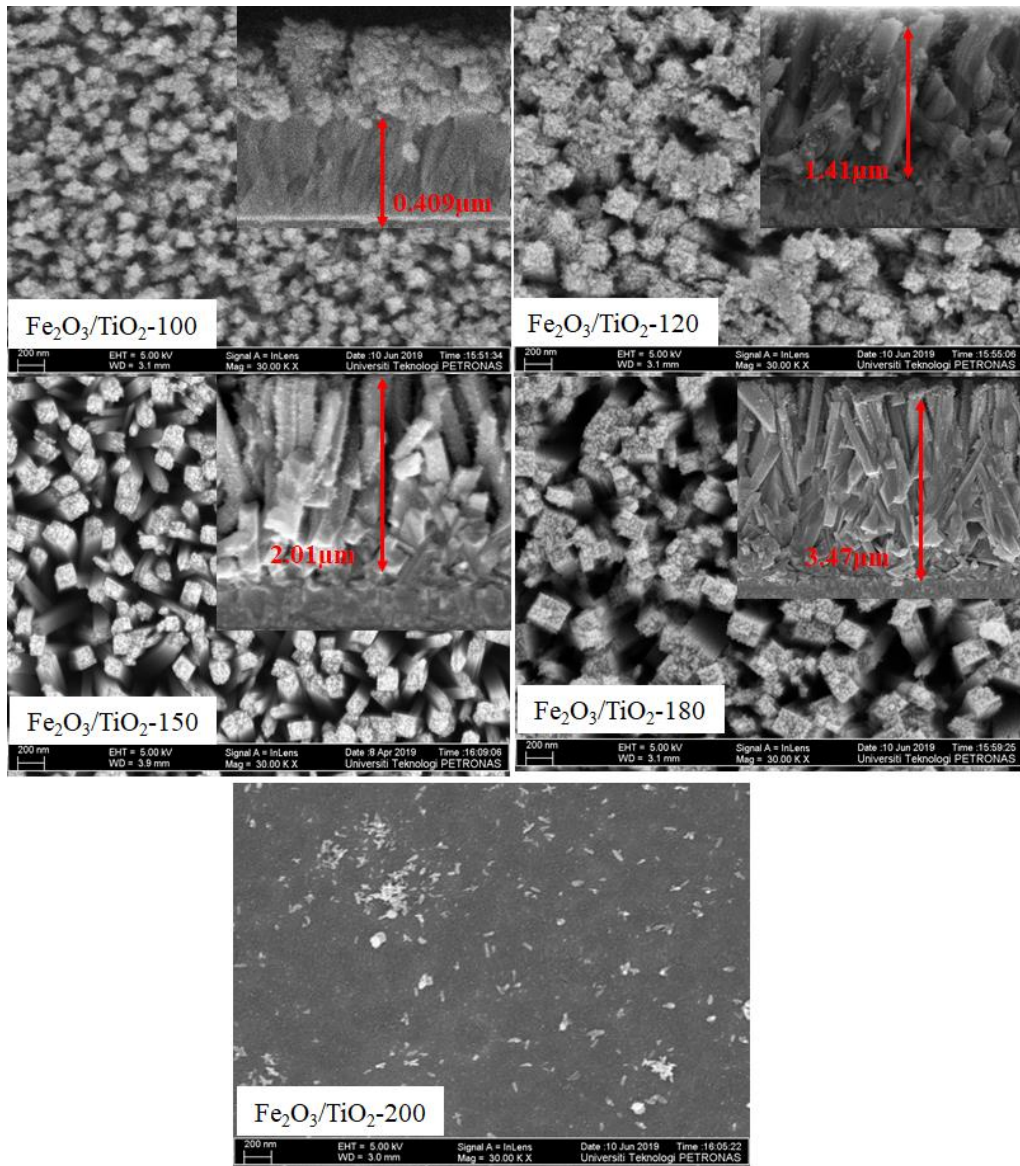
Figure 3. FESEM micrograph images of as-developed Fe_2O_3/TiO_2 NRs prepared at different hydrothermal temperatures.

Figure 5 presents the existence of O, Ti and Fe components with uniform distribution are confirmed on the surface of as-developed Fe_2O_3/TiO_2-150 photocatalyst. Moreover, these results approve that the preparation process did not add any impurities to the structure of Fe_2O_3/TiO_2 nanorod photocatalyst.
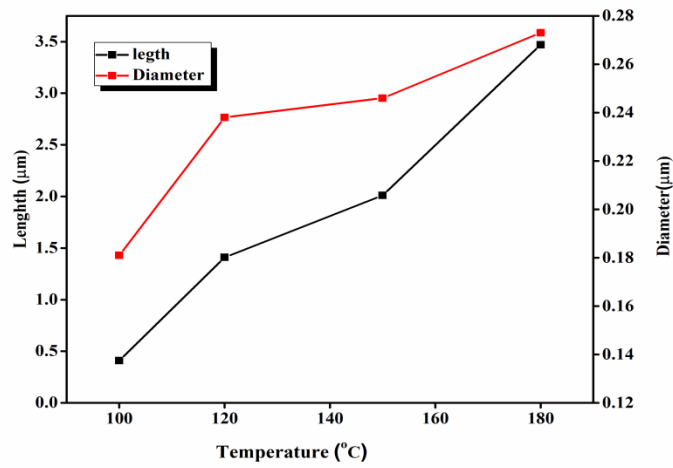
**Figure 4.** Average diameter and length of Fe_2O_3/TiO_2 nanorods at different temperatures.
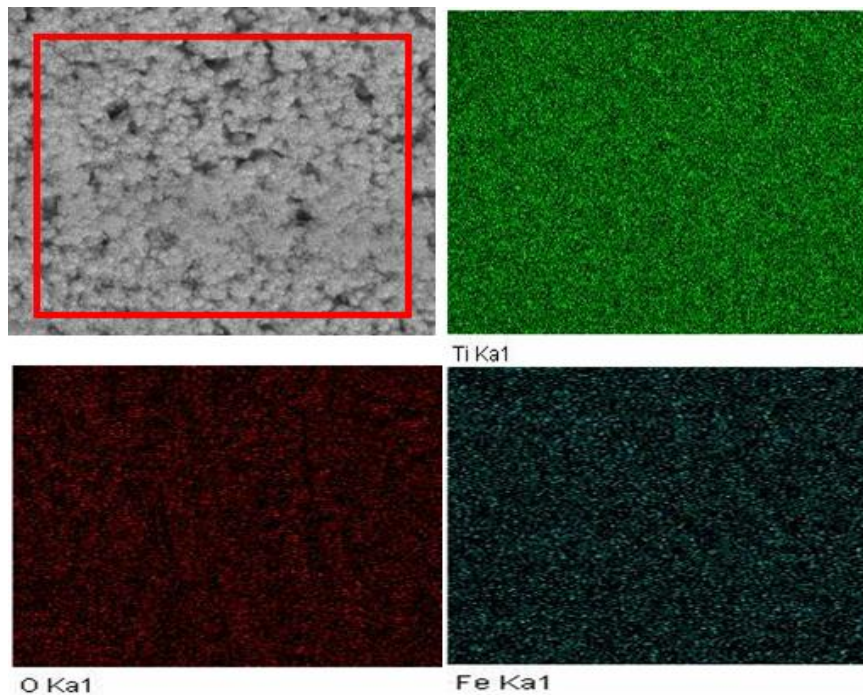
Figure 5. EDX spectrum and the presence of element distribution of the Fe_2O_3/TiO_2-150 photocatalyst

3.2. Optical Absorption Properties

Figure 6(a) displays an optical absorption spectra of Fe_2O_3/TiO_2 hydrothermally grown at different temperatures (100 to 180°C). It is clear that increasing hydrothermal temperature up to 180°C

had a positive impact on the absorbance spectra in both UV and the visible regions due to sufficient growth of TiO_2 NR [39]. The spectra of photoluminescence (PL) for all prepared materials are shown in Figure 6(b) which were collected from 200-700 nm. The PL Intensity is attributed to the recombination of photoexcited charge carriers.The existence of broadband around the 450–550 nm confirms the presence of surface states and the self-trapped excites in the rutile phase, causing high recombination rate of photoexcited charge carriers.
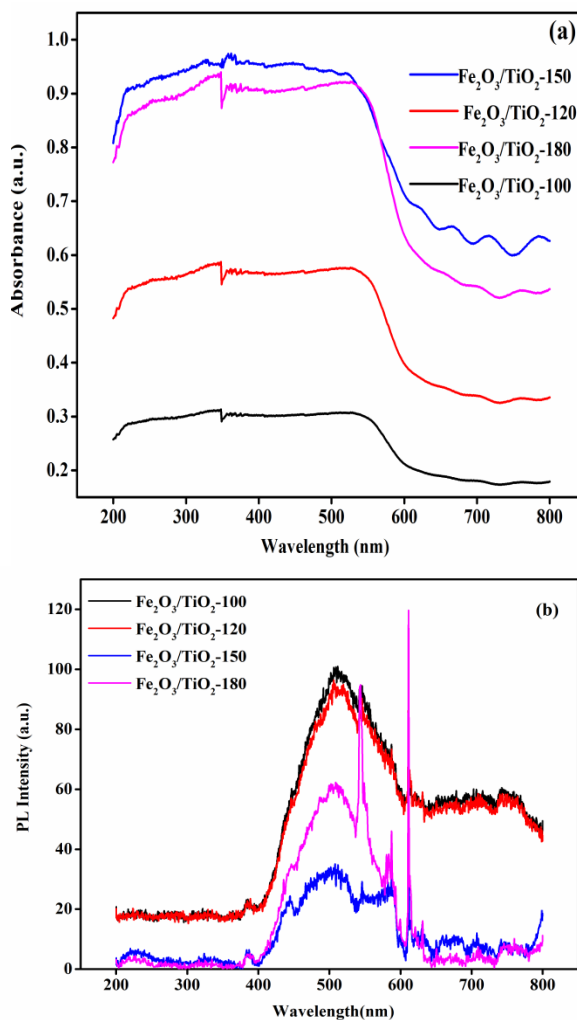

Figure 6.(a) DR-UV-Vis absorption spectra and (b) PL spectra of Fe_2O_3/TiO_2 NRs hydrothermally grown with different temperatures

Also, the existence of a shoulder at about 600–650 nm is an evidence ofthe presenceof the oxygen vacancies in the involved phase. The PL emission intensity of Fe_2O_3/TiO_2 NRs-150 °C is lower than other hydrothermal temperature because of much lower electron-hollow recombination and large effectiveness of separation. Thus, a reduction in the recombination rates of charge carriers causes the

presence of a large number of electrons and photogenerated holes at the electrode/electrolyte interface and improves photocatalytic reaction [24].

3.3. Photoelectrochemical Property

Electrochemical impedance spectroscopy was applied to measure charge carrier resistance and electron lifetime at the surface of electrode/electrolyte of each electrode in open circuit potential (OCP) of the system. Figure 7(a) presents the Nyquist plots of all the prepared photocatalysts in simulated sunlight condition. The equivalent circuit models are Rs $(R_{Pt}Q_{Pt})(R_{Ph}Q_{Ph})$ for all samples. The sheet resistance (Rs) is in series with the parallel charge transfer resistance (Rct) and double-layer capacitance (Q) in the surface of electrodes at the surface of pt as counter electrode and photocatalyst (ph), respectively[16, 25, 26].
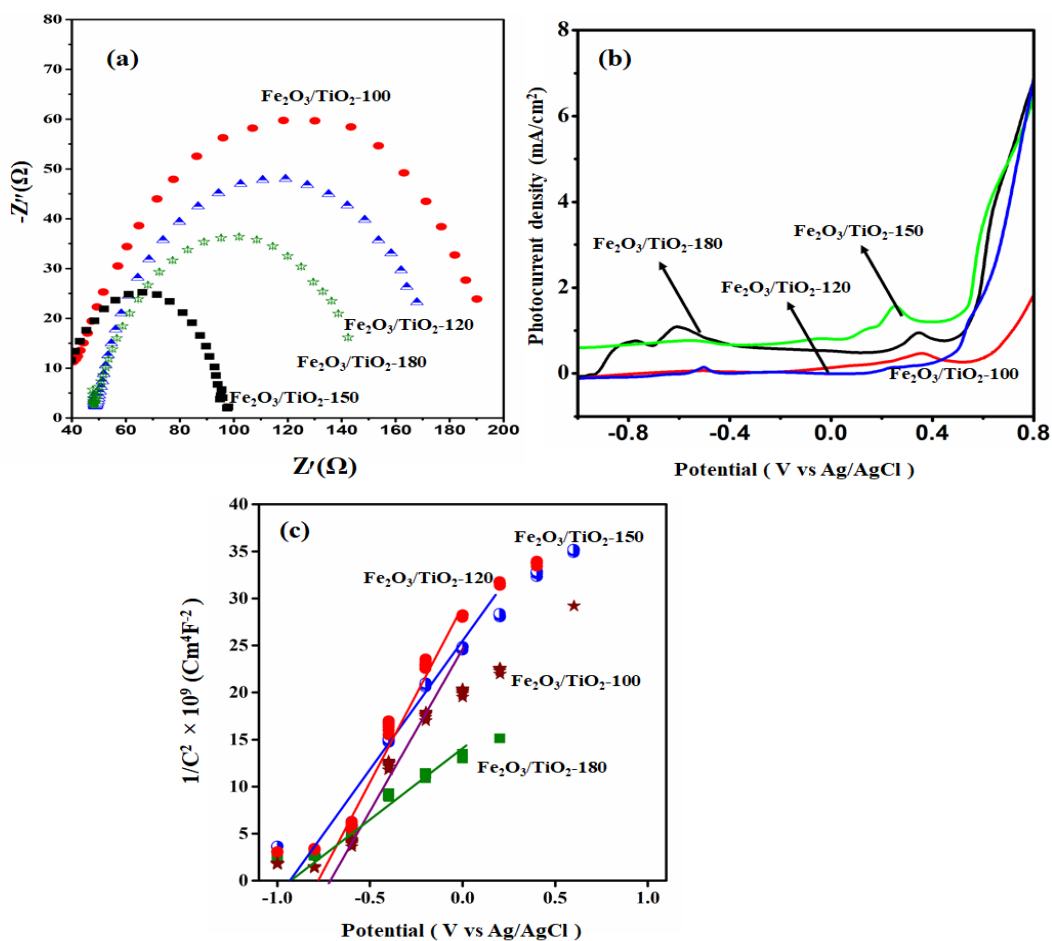
Figure 7.(a)Nyquist plots (b) Photocurrent density, and (c) M-S plots of all prepared photocatalyst at different hydrothermal temperatures

As shown in Figure 7(a) the cell fabricated at 100 °C has the maximum internal resistance of 134.52 Ω with the biggest semicircle and minimum electron lifetime of 140 ms. The semicircle arc and loop diameter were decreased by increasing the hydrothermal temperature up to 150 °C however, further increase in the temperature resulted in increasing the semicircle. The microstructure of the TiO_2 nanorod film strongly controls the charge transfer resistance and electron lifetime at the surface of electrode/electrolyte as confirmed by PL results[27]. Figure 7(b) shows the photocurrent densities of different prepared Fe_2O_3/TiO_2 nanorod at different hydrothermal temperature. These results show the maximum current density is related to the prepared photocatalyst at 150 °C with the lowest semicircle arc and charge transfer resistance at the surface of photocatalyst which can help theexistence of more electrons at the electrode/electrolyte interface.

Figure 7(c) illustrates the Mott-Schottky plots ($1/C^2$ vs. V) of all photoanodes with positive slopes as expected for *n*-type semiconductors. The decreasing slopes from 100 to 150 °C confirm an improvement in charge carrier densities (ND) and negative shift of the flat band (Vfb) as shown in Table 1. It is notable to mention that a photocatalyst with more negative Vfb and high ND show better photocatalytic hydrogen production owing to the presence of more charge carriers at the electrode and the electrolyte interface.

Table 1. ND and Vfb from M-S plots

Hydrothermal Temperature (°C)	N_D (cm^{-3})	V_{fb} (V)
Fe_2O_3/TiO_2-100	1.47×10^{19}	-0.7
Fe_2O_3/TiO_2-120	2.71×10^{19}	-0.8
Fe_2O_3/TiO_2-150	8.45×10^{20}	-0.91
Fe_2O_3/TiO_2-180	7.07×10^{20}	-0.89

Here, we compared the performance ofFe_2O_3/ TiO_2-150 as the best photocatalyst with the literatures as shown in Table 2. However, the comparison of this photocatalyst with relevant past works is difficult due to the facts that we were using different photoanodes and reaction conditions.It can be noted that the Fe_2O_3/TiO_2-150 heterocomposite consisting of TiO_2 nanorod through applying external bias 0.7 V in the photoelectrochemical cell comparatively had a better hydrogen production rate compared to TiO_2 powder photocatalyst in the batch reactor system.

Table 2. A summary of the Fe doped TiO_2 for H_2 production

Photocatalyst	Light source and reaction condition	H_2 production(mmol h^{-1})	Ref.
Fe/Ni-TiO_2	UV and visible light, 60% ethanol/water	0.361	[27]
Fe/TiO_2	300 W Xe arc lamp 20%methanol/water	0.14	[28]
Fe/TiO_2	300 W Xe arc lamp methanol/water	0.025	[29]
Fe/TiO2NR	500W halogen lamp 5% methanol/water	85.8	This work

4. CONCLUSION

In summary, we successfully synthesized Fe_2O_3-TiO_2 NRs with different hydrothermal temperatures and investigated its influence on the physiochemical and photoelectrochemical properties of photocatalysts. The hydrogen production results showed the photoelectrochemical and physicochemical properties could strongly impact on solar hydrogen production. The XRD results showed that increasing the hydrothermal temperatures up to 150 ^{o}C had a positive effect on the growth of different rutile phases while further increasewascaused a growth of only (011) rutile plan and the intensity of the rest of the peaks were reduced. The FSEM results confirmed the better growth of the rutile phase towards axial direction as compared to radial direction. The optical properties showed that increasing hydrothermal temperature was causedan increase in oxygen vacancies and harmed charge transfer and electron lifetime as confirmed by the EIS and photocurrent densities. Finally, the prepared photoanode at 150 ^{o}C improved crystallinity, optical properties, charge transfer, electron lifetime, flat band potential, anddonor density with a positive influence on the hydrogen production.

References

1. M. Wang, M. Pyeon, Y. Gonullu, A. Kaouk, S. Shen, L. Guo, S. Mathur, *Nanoscale,* 7 (2015) 10094.
2. J. Nowotny, C.C. Sorrell, T. Bak, L.R. Sheppard, *Sol Energy.* 78 (2005) 593.
3. W.J. Ong, L.L. Tan, Y. H. Ng, S.T. Yong, S.P. Chai, *Chem. Rev.,*116 (2016) 7159.
4. R. Singh, S. Dutta, *Fuel,*220 (2018) 607.
5. A. Fujishima, K. Honda, *Nature,*238 (1972) 37.
6. M. Kazuhiko, *J. Photochem. Photobiol. C.*, 12 (2011) 237.
7. K. Maeda, N. Murakami, T. Ohno, *J. Phys. Chem. C.*, 118 (2014) 9093.
8. J. Kou, C. Lu, J. Wang, Y. Chen, Z. Xu, R.S. Varma, *Chem. Rev.*, 117 (2017) 1445.
9. W.J. Lee, P.S. Shinde, G.H. Go, E. Ramasamy, *Int. J. Hydrog. Energy,* 36 (2011) 5262.
10. T. Bak, J. Nowotny, M. Rekas, C.C. Sorrell, *Int. J. Hydrog. Energy,* 27 (2002) 991.
11. R. Bashiri, N.M. Mohamed, C. Fai Kait, S. Sufian, M. Khatani, *Int. J. Hydrog. Energy*, 42 (2017) 9553.
12. X. Zhang, Q. Liu, *Mater. Lett.*, 62 (2008) 2589.
13. J. Tian, Z. Zhao, A. Kumar, R.I. Boughton, H. Liu, *Chem. Soc. Rev.*, 43 (2014) 6920.
14. M. Ge, C. Cao, J. Huang, S. Li, Z. Chen, K.-Q. Zhang, S.S. Al-Deyab, Y. Lai, *J. Mater. Chem. A.*, 4 (2016) 6772.
15. C. Cao, C. Hu, W. Shen, S. Wang, S. Song, M. Wang, *Mater. Res. Bull.*, 70 (2015) 155.
16. R. Bashiri, N.M. Mohamed, L.Y. Ling, N.A. Suhaimi, M.U. Shahid, S. Sufian, C.F. Kait, S.M. Saheed, *Diam Relat. Mater.*, 94 (2019) 194.

17. R. Bashiri, N.M. Mohamed, C. Fai Kait, S. Sufian, *Int. J. Hydrog. Energy*, 4 (2015) 6021.
18. R. Bashiri, N.M. Mohamed, C. Fai Kait, S. Sufian, S. Kakooei, M. Khatani, Z. Gholami, *Renew Energ*, 99 (2016) 960.
19. L. Wu, H. Yan, J. Xiao, X. Li, X. Wang, T. Zhao, *Ceram. Int.*, 43 (2017) 14334.
20. H. Fu, S. Sun, X. Yang, W. Li, X. An, H. Zhang, Y. Dong, X. Jiang, A. Yu, *Powder Technol.*, 328 (2018) 389.
21. M. Iraj, F.D. Nayeri, E. Asl-Soleimani, K. Narimani, *J. Alloy Compd.*, 659 (2016) 44.
22. Y. Li, M. Zhang, M. Guo, X. Wang, *Rare metals*,29 (2010) 286.
23. R.A. Solano, A.P. Herrera, D. Maestre, A. Cremades, *J. Nanotechnol.*, 2019 (2019) 11.
24. N.M. Mohamed, R. Bashiri, C. Fai Kait, S. Sufian, S. Kakooei, *Int. J. Hydrog Energy*, 40 (2015) 14031.
25. L. Birry, A. Lasia, *Electrochim. Acta*, 51 (2006) 3356.
26. J. Nayak, K. Prabakar, J.W. Park, H. Kim, *Electrochim. Acta*, 65 (2012) 44.
27. T. Sun, J. Fan, E. Liu, L. Liu, Y. Wang, H. Dai, Y. Yang, W. Hou, X. Hu, Z. Jiang, *Powder Technol.*, 228 (2012) 210.
28. F. Wang, T. Shen, Z. Fu, Y. Lu, C. Chen, *Nanotechnology*, 29 (2017) 035702.
29. M.A. Khan, S.I. Woo, O.B. Yang, *Int. J. Hydrog Energy*, 33 (2008) 5345